Near-Threshold Photoionization of Hydrogenlike Uranium Studied in Ion-Atom Collisions via the Time-Reversed Process

Th. Stöhlker,[1,2] X. Ma,[1,3] T. Ludziejewski,[4] H. F. Beyer,[1] F. Bosch,[1] O. Brinzanescu,[2,5] R. W. Dunford,[6] J. Eichler,[7] S. Hagmann,[8] A. Ichihara,[9] C. Kozhuharov,[1] A. Krämer,[1,2] D. Liesen,[2] P. H. Mokler,[1] Z. Stachura,[10] P. Swiat,[11] and A. Warczak[11]

[1]*Gesellschaft für Schwerionenforschung, 64291 Darmstadt, Germany*
[2]*Institut für Kernphysik, University of Frankfurt, 60486 Frankfurt, Germany*
[3]*Institute of Modern Physics, Lanzhou 73000, China*
[4]*The Andrzej Sołtan Institute for Nuclear Studies, 05-400 Świerk, Poland*
[5]*National Institute for Laser Plasma and Radiation Physics, 76900 Bucharest-Magurele, Romania*
[6]*Argonne National Laboratory, Argonne, Illinois 60439*
[7]*Abteilung Theoretische Physik, Hahn-Meitner-Institut Berlin, 14109 Berlin, Germany*
[8]*Kansas State University, Manhattan, Kansas*
[9]*Japan Atomic Energy Research Institute, Tokai-mura Ibaraki 319-11, Japan*
[10]*Institute of Nuclear Physics, 31-342 Cracow, Poland*
[11]*Institute of Physics, Jagiellonian University, 30-059 Cracow, Poland*
(Received 18 August 2000)

Radiative electron capture, the time-reversed photoionization process occurring in ion-atom collisions, provides presently the only access to photoionization studies for very highly charged ions. By applying the deceleration mode of the ESR storage ring, we studied this process in low-energy collisions of bare uranium ions with low-Z target atoms. This technique allows us to extend the current information about photoionization to much lower energies than those accessible for neutral heavy elements in the direct reaction channel. The results prove that for high-Z systems, higher-order multipole contributions and magnetic corrections persist even at energies close to the threshold.

In a first angular-distribution experiment performed at the ESR jet target for bare uranium ions [1], radiative electron capture (REC) was demonstrated to be a powerful tool for precision studies of the photoionization process in the high-Z domain. This study established that even for the highest nuclear charges and relativistic velocities a cancellation between retardation and Lorentz transformation occurs to a large extent for the angular distribution of the emitted radiation, leading to a nearly forward-backward symmetric distribution in the laboratory system. However, significant deviations from this symmetry were found close to 0° and allowed for an unambiguous identification of spin-flip contributions to the differential cross sections, an effect predicted recently [2–4]. In contrast to direct photoionization experiments (for a review, see Refs. [5,6]), we here introduce a deceleration technique in REC to investigate for the first time differential cross sections for photoionization of a high-Z hydrogenlike ion in the low-energy regime. We show that by means of REC, photoionization can be studied even for excited states in high-Z H-like ions and that relativistic corrections and higher multipoles continue to be important in the vicinity of the ionization threshold [6]. Most importantly, no corrections due to photoelectron scattering occurring in solid targets are required. In conventional photoionization studies for high-Z elements, these effects lead to a considerable loss in the definition of an electron emission angle [7], in particular, at lower photon energies. Therefore, in the high-Z regime,

almost none of the few fine structure- and angle-resolved photoionization data can be compared with theory [6]. For the K shell of high-Z neutral atoms, the available data are restricted to photon energies of 270 keV and above. In gaseous targets, the absence of these difficulties for the inverse process allows one to extend photoionization studies to much lower photon energies than is feasible for the direct channel. In particular, by means of REC even the threshold energies are accessible experimentally. Compared to the high-energy regime—where the kinetic energy of the ejected electron is similar or larger than the initial binding energy—there are important differences for photoionization at low energies. At high energies, the photoionization cross section is determined by the photon-electron interaction at small distances from the nucleus, i.e., of the order of the Compton wavelength. At such distances, electron wave functions are point Coulombic and are not affected by screening or correlation effects. Consequently, no differences between neutral or H-like systems are to be expected at high energies. However, in the intermediate- and low-energy domain where the energy of the ejected electron is comparable or lower than the initial binding energy, much larger distances from the nucleus are involved. As a consequence, the electron-electron interaction may considerably alter the angular distribution of the ejected electrons. For high-Z ions at such energies a further interesting issue arises, i.e., the persistence of higher multipole and relativistic corrections to the angular distributions.

In the current Letter, we present a study of photon angular distributions for the time-reversed photoionization process in collisions of bare uranium ions with light target atoms at low beam energies. We are able to extend our knowledge of the photoionization process in high-Z elements to the low (near-threshold) and intermediate energy domain. For this purpose, bare uranium ions were actively decelerated in the ESR storage ring to an energy of 88 MeV/u [8], corresponding to a photoelectron energy of 48 keV in the direct channel. This has to be compared with the ground-state ionization potential in H-like uranium of about 132 keV.

For the experiment, bare uranium ions were injected into the storage ring at an initial energy of 310 MeV/u. In the electron cooler device, the ions were cooled by an electron beam of 200 mA providing U^{92+} ions with a longitudinal momentum spread of about 5×10^{-5}. Up to 10^8 bare uranium ions were stored and cooled, forming a beam with a diameter [full width at half maximum (FWHM)] of 2 mm. After accumulation and cooling, the ions were decelerated to the final beam energy of 88 MeV/u. (For details of the deceleration technique, see [9].)

To register x-ray emission, the atomic physics photon detection chamber at the internal jet target of the ring was used [10]. This environment allows us to view the beam/jet target interaction zone at a multitude of different observation angles with respect to the beam axis. For our current investigation an array of planar germanium detectors, covering observation angles of about 0°, 35°, 60°, 90°, 120°, and 150°, was used. The projectile x rays were registered in coincidence with down-charged U^{91+} ions using a plastic scintillator installed downstream of the reaction chamber behind the next dipole magnet. A sample coincident x-ray spectrum (recorded at 150°) is depicted in Fig. 1. Since REC is the time-reversed photoionization process, the energy of the REC photons in the projectile frame $\hbar\omega_{\mathrm{REC}}$ is given by $\hbar\omega_{\mathrm{REC}} = E_{\mathrm{KIN}} + E_{\mathrm{BIN}}$. Here, E_{BIN} and E_{KIN} correspond, respectively, to the binding energy in the final projectile state and to the kinetic energy of the target electron with respect to the moving projectile (in the present experiment 48 keV). Therefore, REC transitions into the $1s$ ground state (K-REC, $E_{\mathrm{BIN}} \approx 132$ keV) show up at the high-energy part of the spectrum. Note that the low velocity of the decelerated ions results in a reduced broadening of the REC lines due to the momentum distribution of the target electrons (Compton profile). As a consequence the two j fine-structure components $j = \frac{1}{2}$ and $j = \frac{3}{2}$ of the L-REC x-ray line which are separated by 4.5 keV (projectile frame) can now be resolved. This illustrates an additional benefit of the deceleration technique for our current investigations. In contrast, the large line broadening introduced by the Compton profile at higher energies prevents separation of the fine-structure components [8]. The L-shell fine-structure splitting also leads to the energy separation of the two Lyman-α ground-state transitions (Ly-α_2 + **M1**: $2p_{1/2}$, $2s_{1/2} \to 1s_{1/2}$ and Ly-α_1: $2p_{3/2} \to 1_{1/2}$) which constitute the most intense x-ray lines in the spectrum.
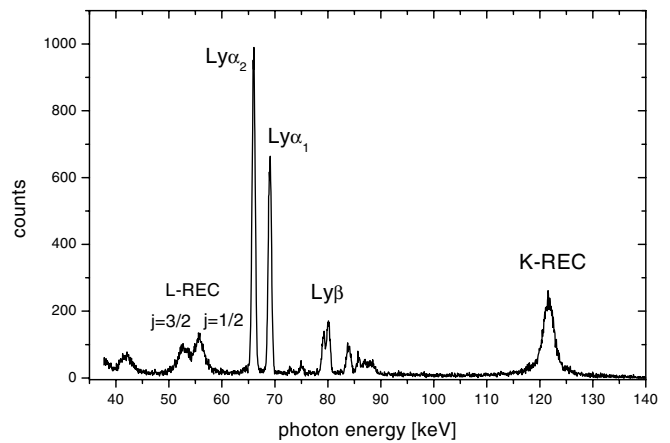

FIG. 1.   Sample x-ray spectrum (laboratory frame) recorded at 150° for $U^{92+} \to N_2$ collisions at 88 MeV/u.

For data evaluation, we adopted the technique discussed in detail elsewhere [8]. Here, all characteristic Lyman ground-state transitions, as well as the REC lines for capture into the K-shell and the L-shell sublevels, were treated by appropriate fitting routines (for details, see [8]). This method was applied to all spectra observed at the different observation angles, except close to 0°. For this particular observation angle, no L-REC transitions were observed. This was due to an intense low-energy background originating predominantly from the forward peaked electron emission produced in the collisions and the resulting bremsstrahlung. In order to derive precise angular emission patterns for the radiative electron capture transitions we exploit the simultaneously observed Ly-α_2 + **M1** radiation. Since we are dealing with spinless ^{238}U nuclei, no hyperfine coupling is present for the H-like projectiles formed by electron capture. Consequently, the Ly-α_2 + **M1** radiation arising from the decay of the $2p_{1/2}$ and $2s_{1/2}$ states is precisely known to be isotropic in the emitter frame. The associated angular distribution in the laboratory frame $d\sigma/d\Omega$ is proportional to $\gamma^{-2}(1 - \beta\cos\theta)^{-2}$ (see, e.g., [11]), where β is the projectile velocity in units of the speed of light, γ is the Lorentz factor, and θ is the observation angle in the laboratory frame. Since β, γ, and θ are precisely known in our experiments, this technique of normalization eliminates almost all possible systematic uncertainties.

In Fig. 2 the experimental results for K-REC are given as a function of the photon emission angle in the laboratory frame (solid circles). In addition, the data are compared with predictions based on rigorous relativistic calculations (solid line) [2,3]. For comparison, the measured angular distribution is normalized to the theoretical prediction at 90°. In Fig. 2, we also display the $\sin^2\theta$ distribution of the nonrelativistic theory (dotted line). For the $1s$ state, this distribution results from the use of nonrelativistic electron wave functions, the inclusion of retardation in the photon wave, and from the Lorentz transformation to the laboratory system. Therefore, deviations of the experimental
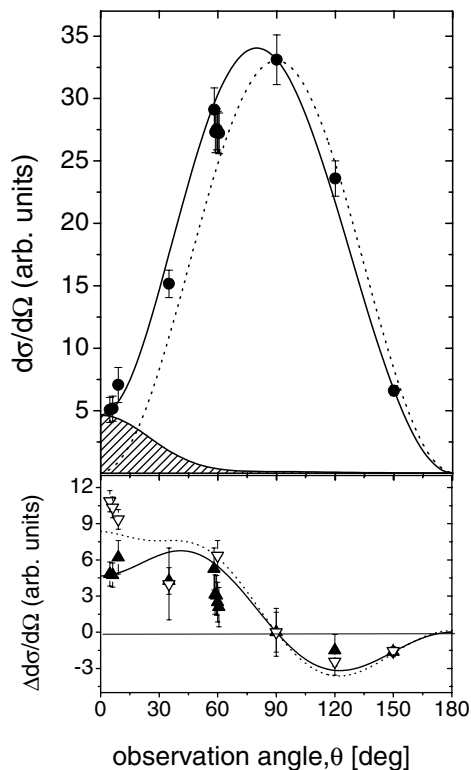
FIG. 2.　Top part:　Angular distributions for K-REC at 88 MeV/u U^{92+} → N$_2$ collisions. Solid circles: experimental result; solid line: relativistic calculations; shaded area: spin-flip contributions; dotted line: $\sin^2\theta$ distribution.　Bottom part: Deviations from the $\sin^2\theta$ distribution. Solid triangles: current experiment; open triangles: 310 MeV/u U^{92+} → N$_2$ [1]; dashed line and solid line: relativistic predictions for U^{92+} → N$_2$ collisions at 310 MeV/u and 88 MeV/u, respectively.

data from the $\sin^2\theta$ pattern are a direct measure of relativistic corrections. As shown in the figure, these corrections lead to deviations from the nonrelativistic theory which are largest for the forward hemisphere. The apparent asymmetry of the complete relativistic prediction with respect to 90° seems to be in accordance with the experimental findings. Most remarkably, the nonvanishing cross section close to 0° proves that magnetic contributions are still present in the low-energy domain. This also emphasizes the high sensitivity of the applied method, since magnetic transitions contribute only 3% to the total K-REC cross section (compare dashed area in Fig. 2).

The difference between the experimental data and the $\sin^2\theta$ distribution is displayed in the bottom part of Fig. 2 ($\Delta d\sigma/d\Omega$). The solid line refers to the deviation of the complete relativistic theory (solid line) from this nonrelativistic prediction. In addition, the corresponding variance is given for the experimental data (open triangles) and the theory for 310 MeV/u U^{92+} → N$_2$ (dashed line), a result published recently [1]. Within the error bars the data sets for both energies are indistinguishable except close to 0°. For angles larger than 40° the corresponding rigorous relativistic descriptions also show only a small energy dependent variation. Consequently, for the energy regime under

consideration, deviations from the nonrelativistic description appear quite energy insensitive and hence are caused by the relativistic wave functions of the high-Z system. Only the spin-flip transitions exhibit a strong velocity dependence caused by the magnetic field originating from the projectile motion (compare region close to 0° in the figure). Note these findings are a specific feature of our reference system, i.e., the laboratory frame. Here, a partial cancellation of retardation and Lorentz transformation occurs as already predicted by the nonrelativistic theory [12]. However, in the emitter frame a strong variation of the angular distribution as a function of energy is present. In Fig. 3 the experimental results are given for the emitter frame. These data are derived from the laboratory system by performing the transformation of the observation angles and solid angles. Although we are dealing with the low-energy domain, the angular distribution still exhibits a considerable backward peaking corresponding to a forward bending of the electron emission distribution for the direct photoionization process. The latter is obtained by interchanging θ' by $\pi - \theta'$ (compare upper x axis in Fig. 3). To facilitate a comparison with an angular distribution for high energies, the results obtained recently by 310 MeV/u

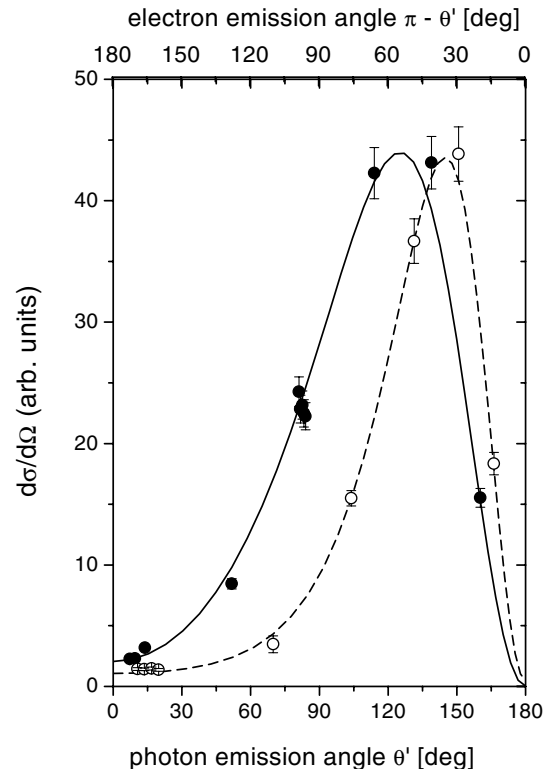FIG. 3.　K-REC distribution (solid circles) in the emitter frame as a function of the emission angle θ' (bottom x axis). The x axis at the top refers to the corresponding electron emission angle in photoionization of U^{91+} (photoelectron energy: 48 keV). The full line refers to a complete relativistic calculation. The result of a former experiment (open circles) conducted at the high energy of 310 MeV/u (photoelectron energy of 170 keV) along with the corresponding theoretical prediction (dashed line) is shown in addition (compare text) [1].

for $U^{92+} \rightarrow N_2$ collisions are displayed in addition by normalizing the maximum of the distribution to the corresponding maximum obtained at the low energy.

A very important aspect of the current study is the improved photon energy resolution caused by the reduced influence of target Compton profiles at low beam energies. We were thus able to derive the j-subshell specific differential cross sections for photoionization of the first excited states in hydrogenlike uranium. These data are shown in Fig. 4. The solid points refer to capture into the two $j = \frac{1}{2}$ fine-structure components of the L shell ($2s_{1/2}$ and $2p_{1/2}$). The open circles give the data obtained for the $2p_{3/2}$ state. The corresponding result of rigorous relativistic calculations is displayed in addition in the figure (full line: $2s_{1/2}$ and $2p_{1/2}$; dotted line: $2p_{3/2}$). The theoretical distribution for the $2s_{1/2}$ state is depicted separately by the dash-dotted line in Fig. 4. The differential cross section observed for the experimentally isolated $2p_{3/2}$ level exhibits a much more pronounced backward shift. Its maximum shows up at angles quite similar to those observed for the K-REC distribution measured at the much higher energy of 310 MeV/u (compare Fig. 3). This illustrates that retardation corrections depend critically on the angular momentum of the 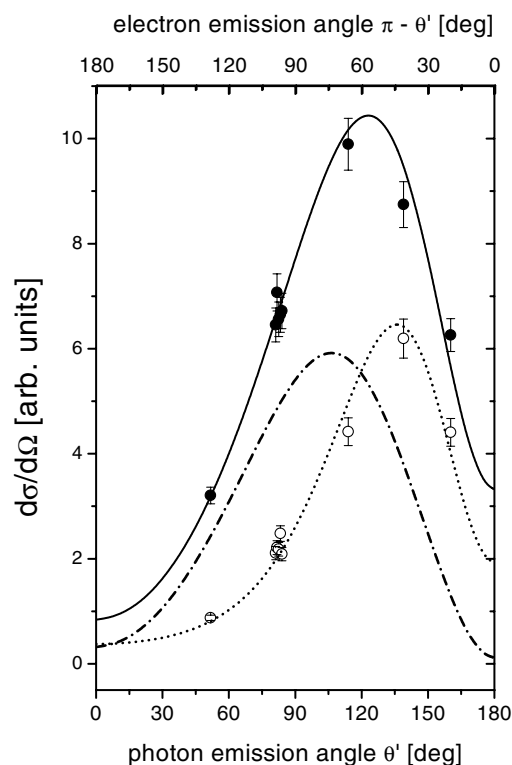final state and that they are much more pronounced for p than for s states. Moreover, for p states, the presence of a nonzero orbital angular momentum leads to a large cross section at 180°. This is in obvious contrast to the displayed distributions for s states (compare Figs. 3 and 4) where only magnetic transitions can produce nonvanishing cross sections at the forward ($\theta' = 0°$) or backward ($\theta' = 180°$) angle. Also, it is interesting to note the difference of our findings to what has been observed in recent soft x-ray photoionization experiments for low-Z atoms where both s and p states show similar sized nondipole effects. Here and in contrast to our present study relativistic corrections can be neglected but electron-electron interaction plays a considerable role [13].

In summary, we introduced the deceleration technique for angular-distribution studies of radiative electron capture into bare uranium ions, i.e., at energies far below the energy required for the production of such high projectile charges. By this technique, we succeeded for the first time to obtain differential cross sections for photoionization of a high-Z hydrogenlike ion in the low-energy regime. The data elucidate the role of retardation effects and magnetic contributions for the low- and intermediate-energy domains and prove the influence of the final-state orbital angular momentum on the associated angular distributions.

FIG. 4.   Angular distribution for the first excited states of U^{91+} observed in $U^{92+} \rightarrow N_2$ collisions at 88 MeV/u (solid circles: $2s_{1/2}$ and $2p_{1/2}$; open circles: $2p_{3/2}$). The lower x-axis refers to the emitter frame whereas the upper scale refers to the corresponding electron emission angle for photoionization. The lines depict the result of relativistic calculations (compare text).

[1] Th. Stöhlker *et al.,* Phys. Rev. Lett. **82**, 3232 (1999); **84**, 1360 (2000).
[2] A. Ichihara, T. Shirai, and J. Eichler, Phys. Rev. A **49**, 1875 (1994).
[3] J. Eichler, A. Ichihara, and T. Shirai, Phys. Rev. A **51**, 3027 (1995).
[4] A. Ichihara, T. Shirai, and J. Eichler, Phys. Rev. A **54**, 4954 (1996).
[5] R. H. Pratt, A. Ron, and H. K. Tseng, Rev. Mod. Phys. **45**, 273 (1973).
[6] H. K. Tseng, R. H. Pratt, S. Yu, and A. Ron, Phys. Rev. A **17**, 1061 (1978).
[7] S. J. Blakeway *et al.,* J. Phys. B **16**, 3752 (1983).
[8] Th. Stöhlker *et al.,* Phys. Rev. A **58**, 2043 (1998).
[9] H. Reich, W. Bourgeois, B. Franzke, A. Kritzer, and V. Varentsov, Nucl. Phys. **A626**, C147 (1997).
[10] Th. Stöhlker, O. Brinzanescu, A. Krämer, T. Ludziejewski, X. Ma, P. Swiat, and A. Warczak, in *X-Ray and Inner Shell Processes,* AIP Conf. Proc. No. 506, edited by D. S. Gemmel, E. P. Kanter, and L. Young (AIP, New York, 1999), p. 389.
[11] J. Eichler and W. E. Meyerhof, *Relativistic Atomic Collisions* (Academic Press, San Diego, 1995).
[12] E. Spindler, H.-D. Betz, and F. Bell, Phys. Rev. Lett. **42**, 832 (1979).
[13] A. Derevianko *et al.,* Phys. Rev. Lett. **84**, 2116 (2000).